

## Supporting Information

### Reversible coupling of radical pair spin dynamics to a locally excited electronic singlet state

Ulrich E. Steiner

Department of Chemistry University of Konstanz, Universitätsstraße 10, 78464  
Konstanz, Germany

E-mail: [ulrich.steiner@uni-konstanz.de](mailto:ulrich.steiner@uni-konstanz.de)

#### Contents

S1	Effect of kinetic coupling to S1 on oscillating CSS decay .....	2
S2.	Accounting for spin effect on CSS recombination in classical model .....	3
S3	Extension of Fig 4.....	5
S4.	Simulating quantum beat case from literature .....	6
S5	Influences of kinetic coupling parameters to S <sub>1</sub> .....	7

## S1 Effect of kinetic coupling to S<sub>1</sub> on oscillating CSS decay

In Fig. S1 we demonstrate the kinetic effect of kinetic coupling to S<sub>1</sub> on S-CSS population for the case without direct singlet or triplet recombination of the CSS. Without that coupling the S-CSS population exhibits coherent oscillations as dictated by the special characteristic of the spin Hamiltonian, in the present example (cf. Fig. S1) only isotropic hyperfine coupling to a single nitrogen nucleus.

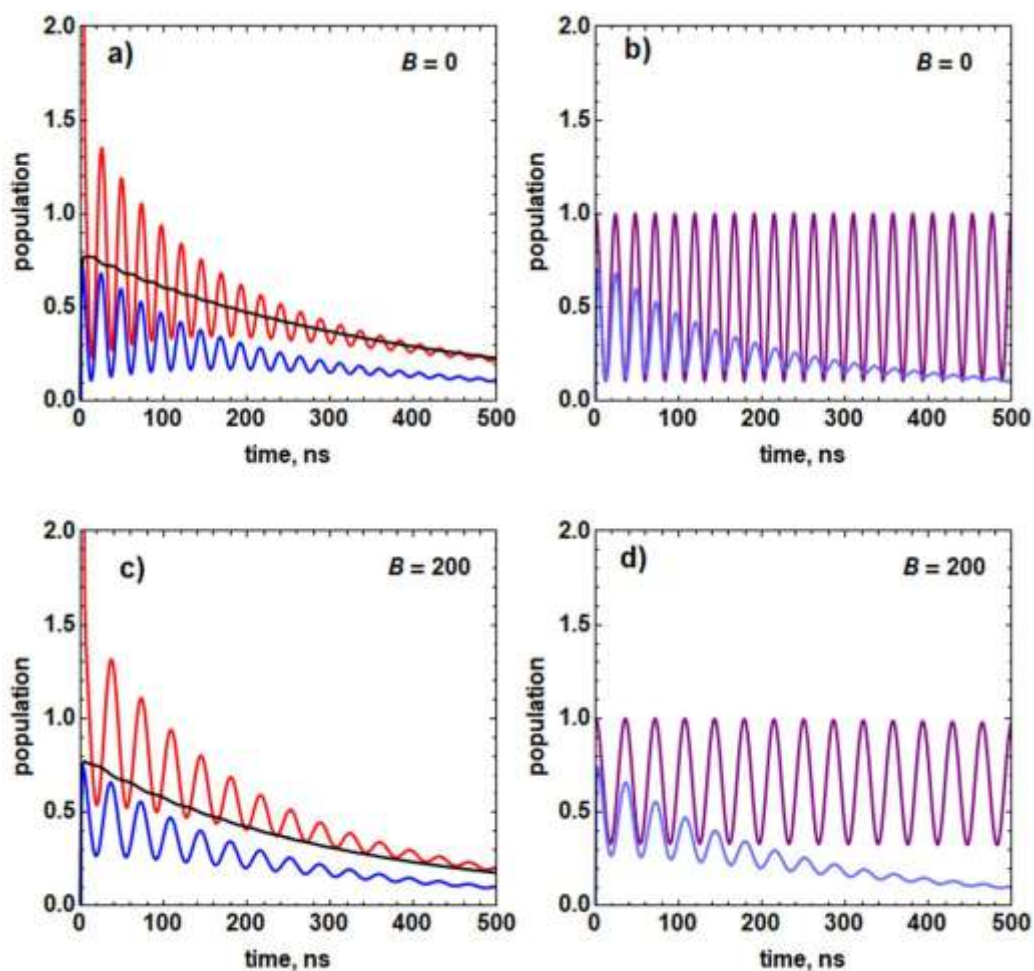


**Fig. S1** Supplement to Fig. 3 (left column corresponds to first row in Fig. 3), right hand column: (purple) S-CSS state evolution, if uncoupled from S<sub>1</sub>. (blue) S-CSS state evolution if coupled to S<sub>1</sub> with coupling parameters given in Table 1.

## S2. Accounting for spin effect on CSS recombination in classical model

In Fig. 3 c) and d), the decay rate of the CSS under spin-dynamic conditions was related to the decay rate under spin-invariant conditions, i.e. without S/T mixing which is given by the expression (eqn (26))

$$k_{slow,0} = \frac{k_f k_{rCS}}{k_f + k_{rCS} + k_{CS}} \quad (32)$$

It represents the decay rate constant in the case where the CSS always remains in the S-CSS substate after its formation. The decay rates under spin dynamic conditions were given as fractions of  $k_{slow,0}$  (cf. legend to Figure S2). Here we show that these fractions represent the average singlet character during the CSS decay.

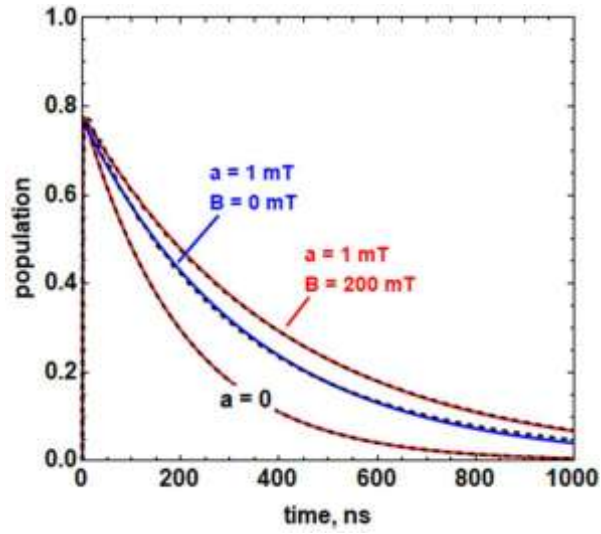


**Fig. S2** CSS decay curves under various conditions. Solid lines according to full quantum dynamical calculation. Dashed lines mono-exponential fits with rate constants  $0.0492 = k_{slow,0}$  ( $a = 0$ ),  $0.0245 = 0.50 k_{slow,0}$  (case  $a = 1$  mT,  $B = 0$  mT) and  $0.0295 = 0.60 k_{slow,0}$  (case  $a = 1$  mT  $B = 200$  mT).

The CSS recombination rate through  $S_1$  fluorescence should be proportional to the population of S-CSS. In case of active spin dynamics, however, the latter undergoes wide amplitude oscillations, that are smoothed out in the decay of CSS. Therefore it is more appropriate to compare the time-accumulated average populations of CSS and S-CSS, viz.

$$\langle \text{CSS} \rangle_t = \frac{1}{t} \int_0^t p_{\text{CSS}}(t) dt \quad (S1)$$

and

$$\langle \text{S-CSS} \rangle_t = \frac{1}{t} \int_0^t p_{\text{S-CSS}}(t) dt \quad (S2)$$

where  $p_{\text{CSS}}(t)$  and  $p_{\text{S-CSS}}(t)$  denote the populations of CSS and S-CSS, respectively.

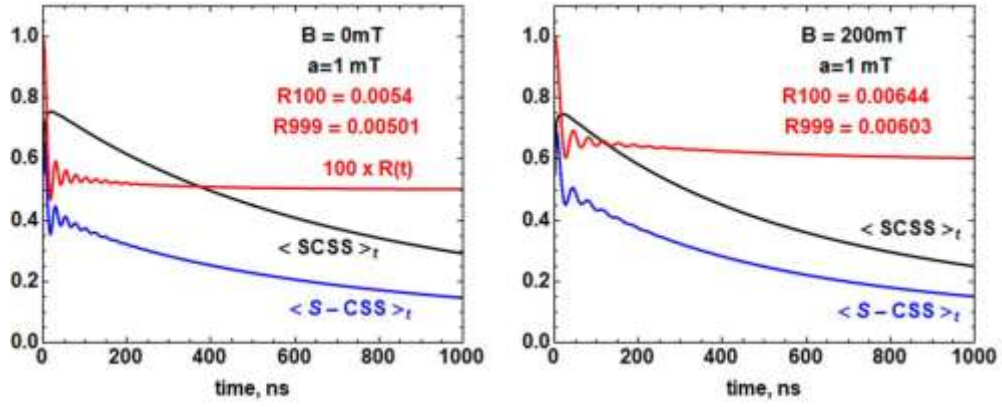


**Fig. S3** Accumulated averages  $\langle \text{CSS} \rangle_t$  of population of CSS (black) and  $\langle \text{S-CSS} \rangle_t$  of population of S-CSS (blue) and their ratio  $R(t)$  for zero field and high field (200 mT).

Choosing 1000 ns for the final  $t$  value where most of the population has decayed, the relative value (cf. Fig. S3)

$$R(t) = \frac{\langle \text{S-CSS} \rangle_t}{\langle \text{C-CSS} \rangle_t} \quad (\text{S3})$$

approaches the factor observed for the reduction of  $k_{\text{slow}}$  by the spin dynamics.

### S3 Extension of Fig 4

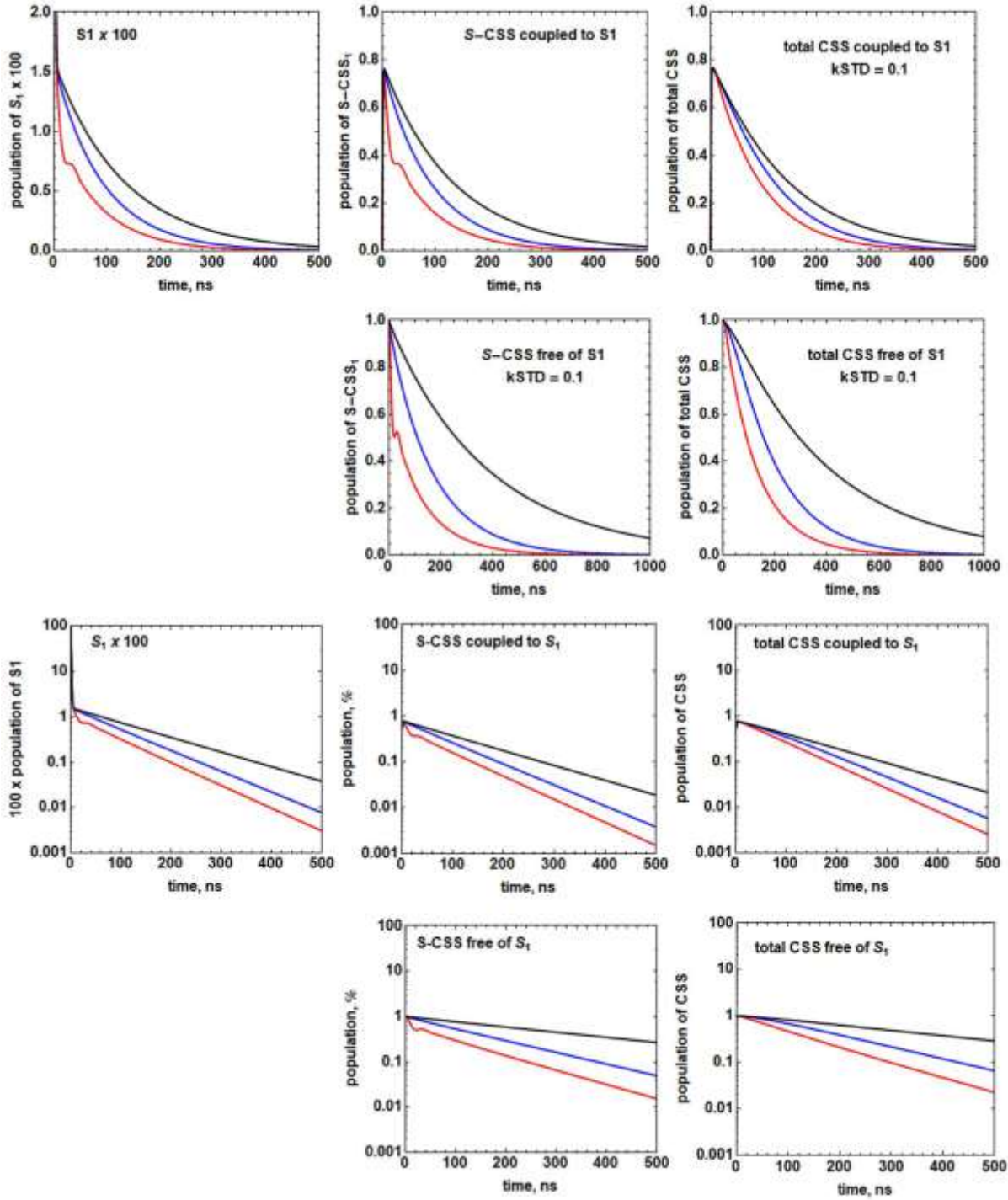
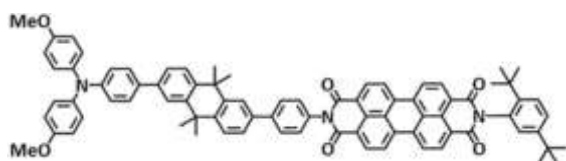


Fig. S4 Linear and log-plots for CSS state coupled or free from  $S_1$ . Parameter set cf. Table 2.

## S4. Simulating quantum beat case from literature

For the triad **TAA-AN-PDI**



the occurrence of quantum beats has been demonstrated by Mims et al., *Science*. 2021;374:1470, using a double laser pulse technique to read out the time dependence of the singlet/triplet character of the CSS. Here we model the hypothetical delayed fluorescence signal assuming a similar kinetic coupling with the  $S_1$  state with pertinent kinetic coupling parameters as given in table 2 in the main paper, but otherwise using the same parameters for the CSS state as in the original work, viz. by applying the following set of parameters: The results are given in Figure S5.

With the  $k_{rCS}$  value chosen approximately as in the realistic case of the parallel experimental paper, the T-CSS populations are only little reduced by the kinetic coupling to  $S_1$  relative to the uncoupled case. The  $S_1$  signal, with its intensities complementary to the population of the T-CSS, shows the full modulation

**Table S1** Set of parameters used to mimic the hypothetical DF in TAA-An-PDI

$k_{CS}$	$k_{rCS}$	$k_f$	$k_S$	$k_T$	$k_{STD}$	$\tau$	$2J$ , mT	$\Delta A$ , mT	$a$ , mT
1	0.025	0.25	0.0095	0.0035	0	0.6	0.7	1.5	0926

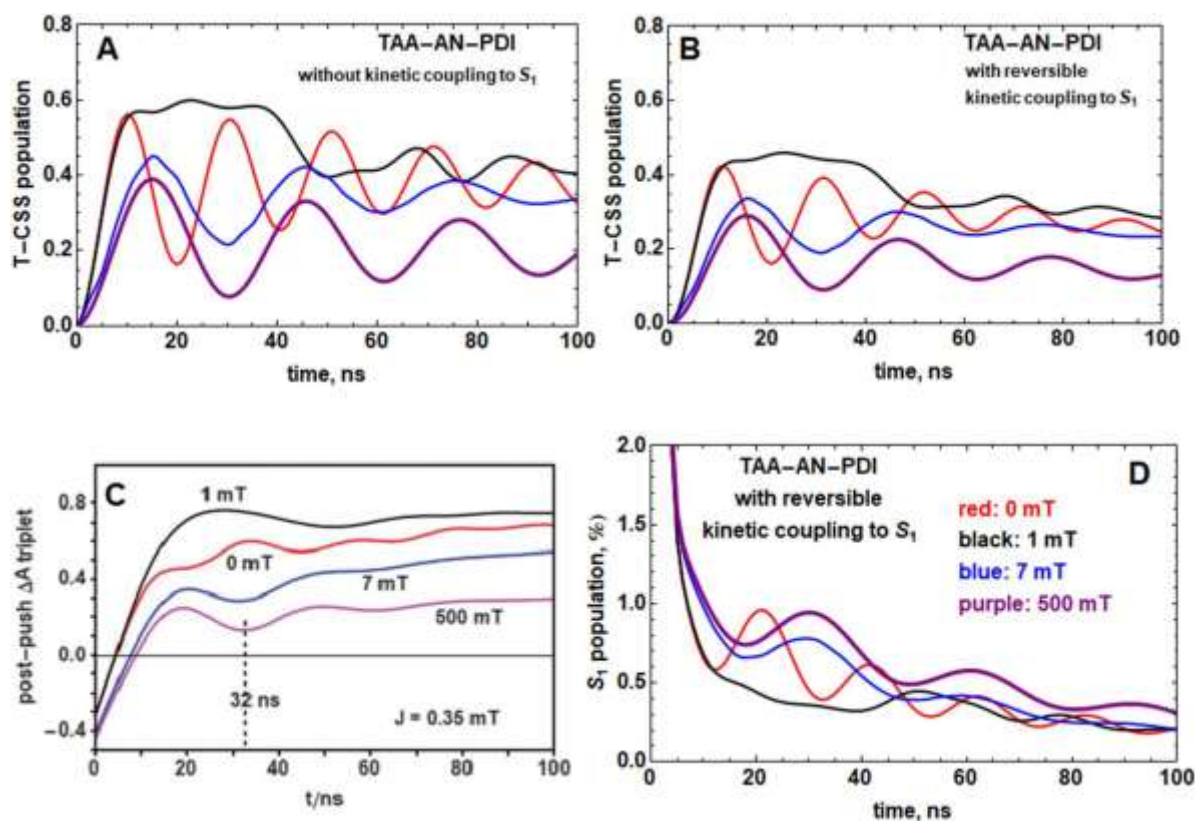


**Fig. S5** Simulation of hypothetical TADF scenario for TAA-An-PDI. Signals shown in panels A – C represent T-CSS population, in panel D  $S_1$  population (%) at fields of 0, 1, 7, 500 mT. Left column kinetics without coupling to  $S_1$ , right column kinetics under conditions of reversible coupling to  $S_1$ . Diagram C represents a diagram from the original paper. It differs from the present calculations by additionally taking into account hyperfine coupling with four hydrogen atoms and by convoluting the signal with the finite laser pulse shape, the latter causing the main difference.

## S5 Influences of kinetic coupling parameters to $S_1$

To study the influence of the  $S_1$ -related kinetic parameters  $k_f$ ,  $k_{CS}$ , and  $k_{rCS}$  the decay signals of  $S_1$ , CSS, and S-CSS and the ratio of  $S_1$  and S-CSS were simulated under variation of the related parameter values. The results are shown in Fig. 5. From the diagrams with higher time resolution it is apparent that there is a phase shift between the  $S_1$  signal and the S-CSS population. The values of phase shifts and decay constants are given in the diagrams and discussed in the figure caption.

### Variation of $k_{CS}$ :

Upon increase of  $k_{CS}$  the decay time of the signals increases. This is in line with the classical model, predicting  $k_{slow}$  in the limit of  $k_{slow} \ll (k_f + k_{CS} + k_{rCS})$  to follow the relationship

$$k_{slow,0} = \frac{k_f k_{rCS}}{k_f + k_{CS} + k_{rCS}} \quad (32)$$

At zero magnetic field (the case shown in Fig. 5), the actual decay rate constant amounts to only 50% of the value predicted by Eq. (26). This reduction accounts for the decreased singlet character of the CSS resulting from S/T conversion, an effect that is not included in the classical model (cf. Section S2).

The ratio of  $S_1$  to S-CSS decreases with decreasing  $k_{CS}$ . This behavior arises from the shift in the equilibrium constant, which is determined by the ratio  $k_{rCS}/k_{CS}$ .

In all plots shown with increased temporal resolution, a phase shift between the  $S_1$  and S-CSS populations is observed. This phase shift increases as  $k_{CS}$  decreases and reflects the delayed response of the  $S_1$  population to oscillations in the S-CSS population. According to classical kinetic theory, the rate constant governing the establishment of equilibrium between two species is given by the sum of the forward and reverse rate constants, i.e.,  $k_{CS} + k_{rCS}$  in the present case. Consequently, faster equilibration results in a smaller phase shift. There is no effect of  $k_{CS}$  on the damping rate of the oscillation, which remains about twice as high as the decay constant for all cases shown.

#### **Variation of $k_{rCS}$ :**

Overall, variations in  $k_{CS}$  produce effects opposite to those induced by changes in  $k_{rCS}$ . This is evident in both the overall decay rate constant and the  $S_1$ /S-CSS population ratio. The behavior of the phase shift, however, is different: Changes in  $k_{CS}$  and  $k_{rCS}$  affect it in the same direction, since the equilibration rate—and thus the phase shift—is determined by the sum  $k_{CS} + k_{rCS}$ . A special effect of  $k_{rCS}$  variation is its effect on the damping time constant of the oscillations. As noted in the main text, the rate constant  $k_{rCS}$  has a dephasing effect proportional to it. This effect becomes very clear in the plots. For a value of  $k_{rCS}$  as low as 0.01, the damping constant is slower than the decay constant. In case of  $k_{rCS} = 0.1$  it is clearly larger than the latter

#### **Variation of $k_f$ :**

The overall decay time decreases with increasing  $k_f$ . This dependence originates from the appearance of  $k_f$  in the numerator of Eq. (26). A potentially opposite effect from its occurrence in the nominator is overcompensated by the large value of  $k_{CS}$ . Increasing  $k_f$  lowers the  $S_1$ /S-CSS population ratio by accelerating the depopulation of  $S_1$ . In contrast, the phase shift remains largely unchanged, indicating that it is governed primarily by the equilibration dynamics between  $S_1$  and S-CSS rather than by the decay of  $S_1$  itself.

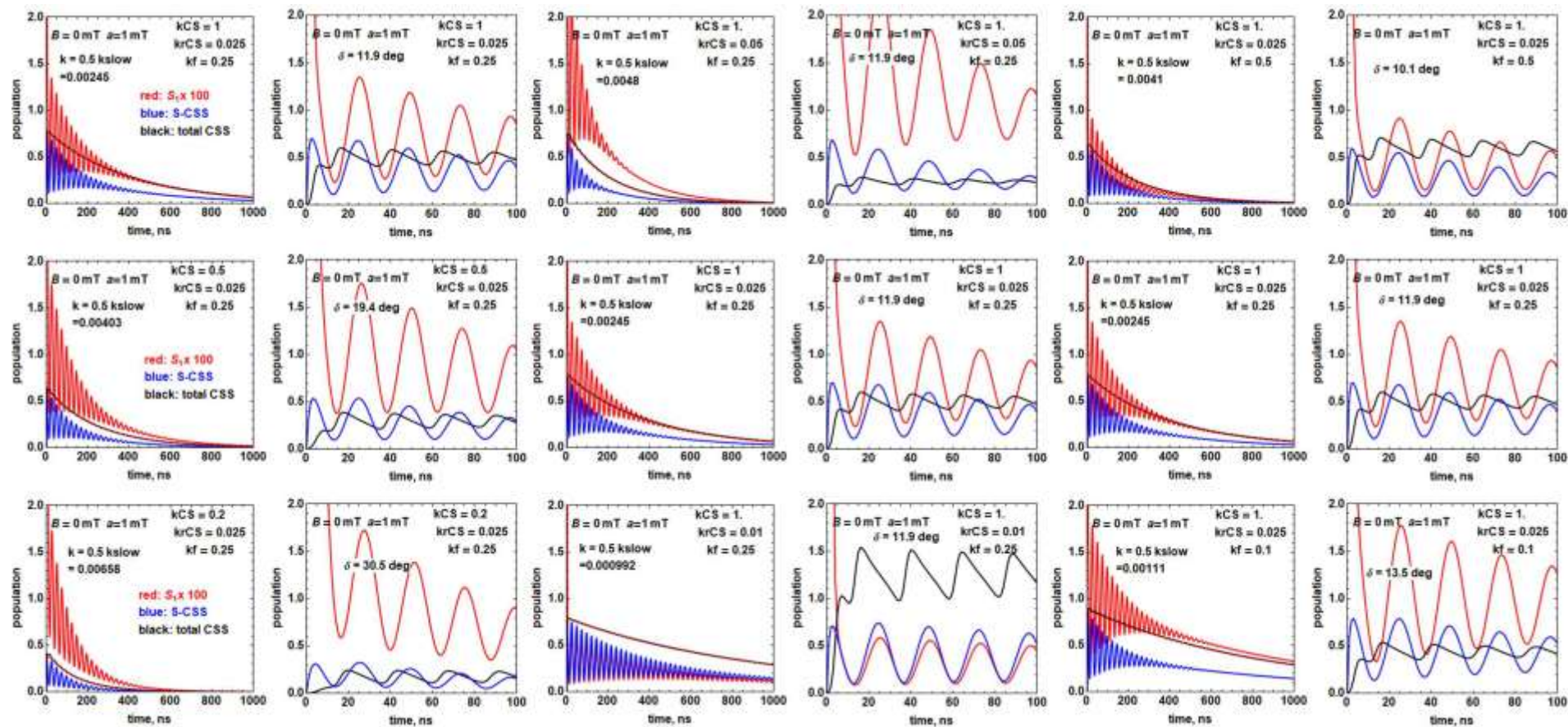


**Fig. 6** Comparing the effects of parameter variation in kinetic coupling to  $S_1$  on  $S_1$  and S-CSS populations. Parameter values that vary are given in the individual diagrams, other parameters as in Table 1 of the main paper. Each pair of columns represents signals of long and short time scale, respectively. The black signal traces in the diagrams with short time scale represents the ratio of population of S-CSS and  $S_1$ , the latter multiplied by a factor of 100.